The Hinge Region between Two Ubiquitin-like Domains Destabilizes Recombinant ISG15 in Solution[†]

Christina M. Sorensen,[‡] Lea A. Rempel,[‡] Shane R. Nelson,[§] Brian R. Francis,[‡] David J. Perry,[‡] Randolph V. Lewis,[§] Arthur L. Haas,[||] and Thomas R. Hansen*,[‡,⊥]

Department of Animal Science and Department of Molecular Biology, University of Wyoming, Laramie, Wyoming 82071, Department of Biochemistry and Molecular Biology, Louisiana State University Health Sciences Center, New Orleans, Louisiana 70112, and Department of Biomedical Sciences, Colorado State University, Fort Collins, Colorado 80523

Received July 12, 2006; Revised Manuscript Received October 19, 2006

ABSTRACT: Interferon-stimulated gene (ISG) 15 mediates antiviral responses and also is upregulated within the endometrium in response to the developing embryo during early pregnancy. Structurally, ISG15 resembles two ubiquitin domains (30% identical) that are separated by a hinge region. Recombinant (r) bovISG15 is not stable in solution. It was hypothesized that the hinge region contributed to the instability of rbovISG15. Within 24 h of dialysis, rbovISG15 formed complexes as detected by reducing and denaturing SDS−PAGE. However, chemical perturbations of cysteine prevented formation of rbovISG15 complexes over time. Furthermore, a site-directed mutant of rbovISG15 (Cys80Ser) was isomeric and more stable than rbovISG15. Neither wild-type nor mutant rbovISG15 was able to interact with the ISG15 E1 initiating enzyme, UBE1L, in an in vitro pull-down assay. Ovine (ov) ISG15 has three additional amino acids within the hinge region that were hypothesized to increase stability and the degree of interaction with UBE1L because of increased separation of the ubiquitin-like domains. Over time in solution, rovISG15 the level of rovISG15 secondary structure was diminished, whereas the Cys80Ser rovISG15 structure did not change. A GST−Cys80Ser rovISG15 fusion protein had increased structural stability and enhanced protein−protein interaction with UBE1L after dialysis for 48 h, when compared to the GST−rovISG15 fusion protein or rbovISG15. Models of bovISG15, Cys80Ser bovISG15, and ovISG15 were constructed, which confirmed that the hinge region between the two ubiquitin domains destabilizes rbovISG15 in solution.

Ubiquitin is a conserved 76-amino acid polypeptide (8.6 kDa) that is involved in an array of post-translational modifications that affect cell cycle regulation, DNA repair, receptor modification, signal transduction, antigen presentation, the stress response, and both proteasomal and nonproteasomal protein degradation (*1*−*3*). Aberrations in protein ubiquitination are associated with diseases such as Parkinson's, Huntington's, Alzheimer's, von Hippel Lindau syndrome, Liddle syndrome, Angelman syndrome, and cancer (*1*, *4*, *5*). Modification of target proteins by ubiquitin occurs through a covalent bond between a lysine in the target protein and the C-terminal glycine of ubiquitin. Activation of the ubiquitin pathway requires the ubiquitin-activating enzyme (E1), which activates ubiquitin Gly^{76} via an ATP-dependent step that creates a thiol ester bond with an E1 cysteine residue (*6*). Ubiquitin is then transferred to a cysteine residue on a ubiquitin-conjugating enzyme (E2). Ubiquitin ligases (E3) transfer the ubiquitin from E2 to the targeted protein. Specific E2s and E3s form complexes which selectively target proteins for different pathways (*7*, *8*). Also critical in ubiquitination are deubiquitinating enzymes, which play a role in the cycling of ubiquitin and target proteins within the cell (*9*).

Bovine ISG15[1] resembles two ubiquitin-like domains that are separated by a "hinge" region. Each domain is 30% identical with ubiquitin in terms of amino acid sequence; however, one critical feature is retention of the C-terminal Leu-Arg-Leu-Arg-Gly-Gly amino acid residues (*10*). The C-terminal sequence has been implicated in the formation of an isopeptide bond between the C-terminal Gly and a specific Lys on targeted proteins for both ubiquitin and ISG15 (*11*). ISG15 becomes covalently attached to targeted proteins (ISGylation) using an ATP-dependent and multiple-enzyme process that is distinct from the ubiquitin conjugation pathways. For example, ISG15 has a unique E1 that does not interact with ubiquitin and is called UBE1L (*12*, *13*). The crystal structure of Cys78Ser human ISG15 has been utilized to model the binding of ISG15 to UBE1L (*14*).

[†] The research was supported by NIH Grant HD 32475, NIH INBRE Grant 1P20RR16474, and NIH COBRE Grant P20 RR 015553 (T.R.H.) and by NIH Grant GM 47426 (A.L.H.).

* To whom correspondence should be addressed: Department of Biomedical Sciences, Colorado State University, Fort Collins, CO 80523. Phone: (970) 491-8081. Fax: (970) 491-3557. E-mail: thansen@colostate.edu.

[‡] Department of Animal Science, University of Wyoming.

[§] Department of Molecular Biology, University of Wyoming.

[||] Louisiana State University Health Sciences Center.

[⊥] Colorado State University.

[1] Abbreviations: BME, β-mercaptoethanol; bov, bovine; CD, circular dichroism; GSH, glutathione; GST, glutathione *S*-transferase; IFN, interferon; ISG, IFN-stimulated gene; MALDI-TOF MS, matrix-assisted laser desorption ionization time-of-flight mass spectrometry; ov, ovine; PBS, phosphate-buffered saline; rbov, recombinant bovine; rov, recombinant ovine; Ubl, ubiquitin-like molecule.

10.1021/bi061408x CCC: $37.00
Published on Web 12/21/2006

Although the functional consequences of ISGylation are not fully understood, in response to IFN-τ in ruminants, ISG15 is induced and becomes covalently attached to endometrial proteins during early pregnancy (*15*−*18*). ISG15 and its conjugates are also upregulated in the uterus during pregnancy in mice (*19*), swine (*20*), humans, and baboons (*21*). Some putative targets for ISGylation include serpins (*22*) and signal transduction proteins (*23*, *24*). Many other targets for ISG15 were identified by Zhao et al. (*25*), including structural or functional cytoskeletal proteins, numerous metabolic enzymes, and nuclear proteins which targeted RNA processing.

We have identified the bovine ISG15-activating enzyme, UBE1L (*26*), which functions in mediating the conjugation of ISG15 to targeted proteins (*12*). In vitro confirmation that ISG15 and UBE1L interact relies on the production of stable rISG15 that retains proper structure to allow protein−protein interactions. In addition, unstable rbovISG15 might affect the quality and cross-reactivity of antibodies that are raised against rbovISG15 and are expected to recognize the native free and conjugated ISG15. To mimic in vivo conditions for conjugation of rbovISG15 to proteins, examination of the secondary structure and the effects of oxidation on rISG15 structure in vitro is necessary.

A key feature within the structure of ISG15 is the presence of a Cys residue within the hinge region (residues 76−80 in the native bovine protein). Cysteine 78 is conserved among mice, humans, cows, and sheep ISG15. Narasimhan et al. (*14*) described the crystal structure for the Cys78Ser human ISG15 and demonstrated that disulfide formation through Cys78 destabilized ISG15. In contrast to that of the human, mice, or ovine ISG15, the hinge region for bovISG15 is shorter. Recombinant bovISG15 is not stable over time in solution. Dimers (34 kDa), half-monomers (e.g., 8.5 kDa), and one-and-a-half monomers (26 kDa) were detected on Western blots using anti-ISG15 antibody. Because a conserved cysteine (Cys78 in the native form is Cys80 in rISG15) is located within the hinge region between two ubiquitin-like domains of recombinant (r) ISG15, we hypothesized that this residue contributed to the instability of rISG15 in solution. The stability of rbovISG15, as determined by mass (Western blot and MALDI-TOF mass spectrometry) and structure (circular dichroism spectroscopy), was examined herein following chemical perturbations (site-directed mutagenesis, reduction, carboxyamidomethylation, and oxidation) of this Cys residue. Native ovine ISG15 has three more amino acids present in the hinge region following Cys78 (Cys80 in rovISG15) than are present within the native bovine protein hinge region. It was also hypothesized that the presence of these three amino acids in rovISG15 would help to improve structural stability and function compared to those of rbovISG15. The stability of the recombinant ovISG15 and Cys80Ser rovISG15 was examined by mass (Western blot and MALDI-TOF-MS), structure (circular dichroism spectroscopy), and function (ability to bind UBE1L over time). Secondary structure and hinge region models of bovISG15, Cys78Ser ovISG15, and ovISG15 were also compared with the Cys78Ser human ISG15 crystal structure (*14*) to determine if the hinge region in rbovISG15 destabilized the protein in solution.

EXPERIMENTAL PROCEDURES

Materials

All solvents for mass spectrometry experiments were HPLC-grade (Fisher Scientific, Pittsburgh, PA). Reagents and nitrocellulose membranes (Micron Separations, Westborough, MA) and the Bradford protein assay (Bio-Rad Laboratories, Richmond, CA) were obtained. All other reagents and chemicals were purchased from Sigma Chemical Corp. (St. Louis, MO) or Fisher Scientific.

Methods

Recombinant ISG15 Expression. Recombinant bovISG15 was expressed in Bl21-RIL *Escherichia coli* (*13*, *19*). rbovISG15 was expressed with an Arg C-terminal cap to protect the C-terminal Gly from carboxypeptidase activity during synthesis (*14*). Following expression, the GST−rbovISG15 fusion protein was bound to GSH resin and separated from *E. coli* cellular proteins. The presence of the C-terminal Arg was confirmed within 0.05% of the calculated mass using MALDI-TOF MS (17 610 Da). Carboxypeptidase B treatment removed the C-terminal Arg, and rbovISG15 was cleaved from the GST−GSH protein using thrombin. Confirmation of correctly processed rboISG15 was obtained by MALDI-TOF MS (parent ion mass of 17 455 Da) within 0.05% of the calculated mass, Coomassie-stained one-dimensional PAGE, and Western blot detection. rovISG15 was expressed as described for rboISG15 in *E. coli* (*13*). Analysis by using MALDI-TOF MS confirmed the final mass of rovISG15 (parent ion at 17 645 ± 0.05% Da).

Production of Cys80Ser rISG15 by Site-Directed Mutagenesis. Recombinant Cys80Ser ISG15s were prepared by using site-directed mutagenesis (Gene-Editor Mutagenesis from Promega Corp., Madison, WI). The mutant oligonucleotide (5′-GGTGCAGAACAGCATCTCCA-3′) was designed to hybridize to the bovine ISG15 cDNA (AF069133) within the region encoding the highly conserved Cys80 (in the recombinant protein) with a simple T to A base substitution. Thus, a Ser (AGC) substitution for Cys (TGC) was engineered. Annealing of the oligonucleotide, subsequent synthesis, ligation of the mutant strand of the plasmid, transformation, and selection of mutant colonies were performed as described (Gene-Editor Mutagenesis). Extracts from *E. coli* transformed with Cys80Ser plasmid were either pelleted and stored at 4 °C overnight or lysed immediately and stored overnight at 4 °C prior to purification of the GST−Cys80Ser rbovISG15 fusion protein. The presence of the C-terminal Arg for rbovCys80Ser ISG15 was confirmed by using MALDI-TOF MS (17 594 ± 0.05% Da). The Cys80Ser mutation was confirmed using DNA sequencing, and the final mass of the modified protein was confirmed by Western blot analysis and MALDI-TOF MS (within 0.05% of the calculated parent ion; 17 439 ± 0.05% Da). The rovCys80Ser form was prepared as described for rbovCys80Ser with a final parent ion mass of 17 629.36 ± 0.05% Da.

MALDI-TOF Mass Spectrometry. MALDI-TOF MS (Voyager DE-PRO, Applied Biosystems) was externally calibrated against horse heart myoglobin (16 951 Da) in positive ion mode with delayed extraction. One microgram of the protein solution was mixed with 25 μL of a saturated sinapinic acid matrix solution [20 mg of sinapinic acid in 1 mL of a 50:50

(v/v) water/acetonitrile mixture with 0.1% TFA]. One microliter of the mixture was placed on a stainless steel sample plate (Applied Biosystems), allowed to dry, and rinsed once with water prior to mass spectrometry. All protein samples were analyzed in triplicate under the conditions described above. Spectra (not shown) were 80 averaged laser shots within the *m*/*z* range of 5−50 kDa.

Effect of Reductant on Recombinant ISG15 over Time. Recombinant proteins were freshly prepared, dialyzed against PBS with or without 5 mM β-mercaptoethanol (BME) at 4 and 22 °C for appropriate times (0, 12, 24, and 48 h), placed in 2× Laemmli buffer, heated at 95 °C for 5 min, and frozen at −20 °C until SDS−PAGE and Western blot analysis were performed. These samples were separated via one-dimensional PAGE and electroblotted onto nitrocellulose (0.2 μm) membranes in Towbin buffer. ISG15 and its multimers were detected utilizing murine monoclonal 5F10 anti-rbovISG15 antibody (1:50000) and alkaline phosphatase-conjugated anti-mouse IgG (1:10000; Promega Corp.) as the second antibody (*27*). Immunoreacting bands were visualized by nitro blue tetrazolium and 5-bromo-4-chloro-2-indolyl phosphate substrate solutions (Promega Corp.). Western blots were scanned and quantitated with UNSCANIT (Silk Scientific, Orem, UT). Samples were analyzed in triplicate.

Effects of Long-Term Storage on Recombinant bovISG15. Fresh recombinant proteins were stored in PBS at 4 °C for 18 days (Cys80 and Cys80Ser). One microgram of each protein solution was analyzed by MALDI-TOF MS. Aliquots of the stored solutions containing 1 μg of recombinant proteins were also analyzed with Western blots. Newly expressed rbovISG15 was analyzed immediately in PBS by MALDI-TOF MS. Average parent ions for Cys80 rbovISG15 (17 455 Da) and Cys80Ser rbovISG15 (17 439 Da) were within 0.05% of the calculated masses for these expressed proteins.

Samples (rbovISG15) were also stored at −20 °C for 1 year in PBS in the absence of reductant. One microgram of the protein was analyzed with Western blots. The protein mixture was separated by utilizing a C18 ZipTip (Millipore Corp., Billerica, MA). Briefly, the ZipTip was washed with 55% acetonitrile ten times and equilibrated with a 0.1% solution of trifluoroacetic acid three times; the sample was introduced into the ZipTip ten times, and the proteins were eluted using 65% acetonitrile with 0.1% trifluoroacetic acid. Eluted protein was analyzed with MALDI-TOF MS in linear mode as described earlier using ubiquitin as the internal standard (8565.61 Da).

Structural Characterization of Cys80 and Cys80Ser rbovISG15 and rovISG15 in Solution. Recombinant proteins were dialyzed (molecular mass cutoff of 3500 Da) immediately after preparation against 10 mM sodium phosphate buffer (pH 7.4 and 22 °C) and stored at −80 °C until spectra were collected. A buffer blank was also collected at this time. Two (bovine) or three (ovine) samples from each time point were collected from the pooled dialysis and were analyzed on a JASCO 800 spectropolarimeter in a 0.1 cm thermostated cell at 22 °C and purged during the analysis with nitrogen. All spectra represent the average of five scans from 260 to 180 nm (0.1 nm intervals) that were adjusted for the blank (also five averaged scans).

The Varslc algorithm was used to calculate secondary structure content (*28*) via DICHROWEB (*29*, *30*). Samples from the 0 and 48 h dialyses were analyzed. The corrected spectra were loaded into the program in text format at 1 nm intervals using the full scan from 260 to 180 nm. Data were reported as mean residue ellipticity and percent secondary structure.

Functional Consequences of ISG15 Structure: Ability To Bind Bovine Ubiquitin-Activating E1-like Enzyme (UBE1L). Recombinant GST-fused ovISG15 and GST-fused Cys80Ser ovISG15 were produced, dialyzed (4 and 48 h at 22 °C as described previously), and bound to glutathione−Sepharose columns as described by Rempel (*13*). Confluent bovine endometrial (BEND) cells (ATCC, Manassas, VA) were cultured, and soluble components were extracted. Briefly, the soluble fractions (control and IFN-τ-treated) and 10 mM Mg^{2+} and 2 mM ATP were applied to glutathione−Sepharose columns. Proteins which were covalently attached via thioester bonds to ISG15 were eluted from the columns utilizing 40 mM dithiothreitol (DTT) in 20 mM Tris-HCl (pH 7.5). These protein products were concentrated using 30 000 Da molecular mass cutoff concentrators and separated by one-dimensional SDS−10% PAGE and Western blotted using anti-human UBE1L antibody as described previously (*13*).

Modeling of bovISG15, ovISG15, and Cys78Ser ovISG15. Molecular dynamics analysis for native bovISG15, native ovISG15, and Cys78Ser ovISG15 was performed by threading each sequence on Cys78Ser human ISG15 (PDB entry 1Z2M) utilizing Deep View in conjunction with SWISS-MODEL (*31*). The energy of each system was first minimized at 0 K for 2 ps. The systems were then simulated for 10 ns at 310 K. From each of these trajectories, 100 coordinate sets were collected at 100 ps intervals. Minimization and molecular dynamics analyses were completed using NAMD2 and the force field CHARMM22 (*32*, *33*). Results were visualized utilizing VMD (*34*). Molecular dynamics of the Cys78Ser human ISG15 structure was performed as a negative control of the simulation conditions. Models were submitted to the Protein Data Bank for bovISG15 (2BX0), ovISG15 (2BWZ), and Cys78Ser ovISG15 (2BX1). Secondary structure assignments were averaged for all time steps using STRIDE (*35*).

Statistical Analysis. Effects of time, BME, temperature, and site-directed mutagenesis (Cys80Ser) on the stability (Western blot) and structure (CD spectroscopy) of Cys80 and Cys80Ser rbovISG15 were analyzed by using ANOVA (SAS Institute, Inc., Cary, NC). When ANOVA revealed a significant main effect ($p < 0.05$), means were further analyzed by using a *t*-test.

RESULTS

The masses of capped (C-terminal Arg) rbovISG15 and Cys80Ser rbovISG15 and uncapped (C-terminal Gly) rbovISG15 proteins were determined using MALDI-TOF MS (Figure 1). Mass spectral analysis confirmed removal of the C-terminal Arg and the site-directed mutagenesis of Cys to Ser within 0.05% of the calculated parent mass. After expression, all forms of rbovISG15 migrated to ∼17 kDa on Western blots (data not shown). Recombinant protein dimers (Cys80 or Cys80Ser) were not detected in the MALDI-TOF mass spectrum at the concentrations described when proteins were analyzed immediately after expression.

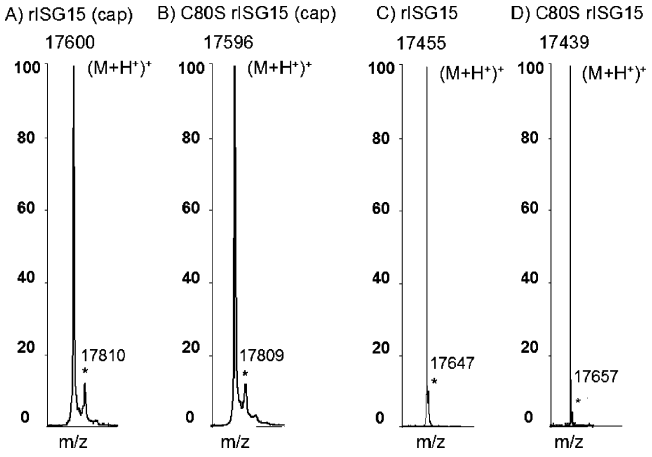

FIGURE 1: Confirmation of rbovISG15 and Cys80Ser rbovISG15 synthesis utilizing MALDI-TOF MS. MALDI-TOF MS analysis of capped rbovISG15 and Cys80Ser rbovISG15 (left two panels) and uncapped rISG15 proteins (right two panels) utilized for confirmation of syntheses. The parent ions shown are within 0.05% of the calculated mass. The asterisk denotes the sinapinic acid adduct.

The stability of Cys80 rbovISG15 was affected by dialysis in 0.25 mM Tris buffer (pH 7.4) (Figure 2A). The purified Cys80 rbovISG15 appeared as a single 17 kDa band on PAGE gels immediately after expression and prior to dialysis (Figure 2A). After storage for several months at −20 °C and following dialysis for 4 h at 4 °C, a 34 kDa band that immunoreacted with anti-ISG15 antibody appeared. Following dialysis for 24 h after storage at −20 °C, an immunoreacting 26 kDa and cleavage product (8.5 kDa) also appeared.

A faint 26 kDa immunoreactive band appeared following dialysis for 48 h at 22 °C in the absence of reductant for Cys80 rbovISG15 (Figures 2 and 3). Increased temperature during dialysis caused an increase in the level of formation of the 34 kDa dimer of rbovISG15 at 12 h from 0% of total protein loaded at 4 °C to 7.9% of protein loaded at 22 °C (Figure 2B,C). Increased temperature and time of dialysis and an absence of reductant caused a greater ($p < 0.0001$) level of formation of the 34 kDa protein for Cys80 rbovISG15 (Figure 2D). After dialysis for 24 h at 4 °C, a dimer (9.6%) appeared for Cys80 rbovISG15. In contrast, Cys80Ser rbovISG15 was not affected by time or temperature of dialysis or by the presence or absence of reductant. Analysis of the reduced (5 mM BME) and alkylated (50 mM iodoacetamide) rboISG15 (Cys80 and Cys80Ser) dialysis products was similar to treatment with BME alone (not shown).

The effect of reductant, time, and temperature on Cys80Ser rbovISG15 was examined by Western blot analysis (Figure 3A). An unexpected additional higher-molecular mass band appeared. This immunoreactive band was the result of 14 amino acids that were added to the C-terminus of Cys80Ser (Figure 3B) because of a lack of recognition of a stop codon within the cDNA for ISG15 and the recognition of a second stop codon immediately downstream within the pGEX-4T-1 cloning vector. When *E. coli* extracts were pelleted and stored at 4 °C, two forms of Cys80Ser rbovISG15 were synthesized (see the doublet in Figure 3A). The mass spectrum for this protein (Figure 3B) showed that multiple forms were due to different protein processing. However, when *E. coli* extracts were lysed immediately and stored at 4 °C, only the 17 kDa

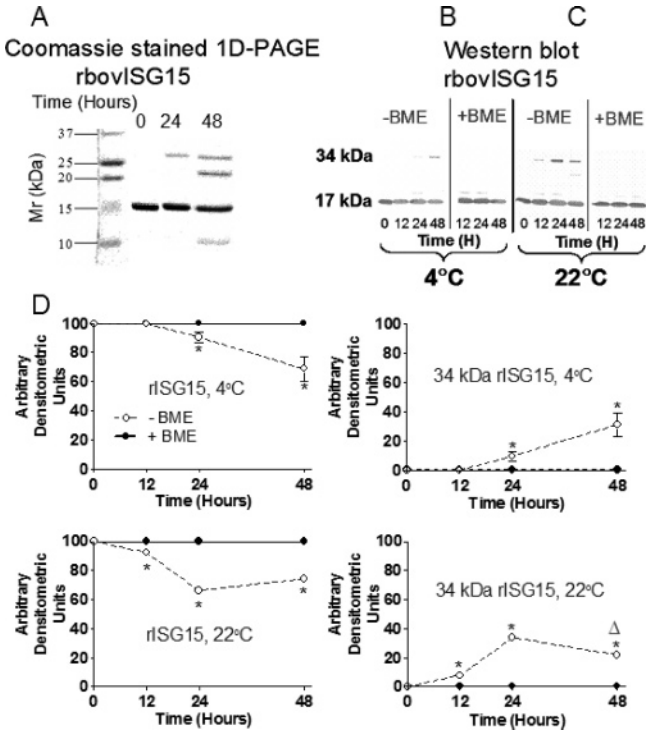

FIGURE 2: Stability of rbovISG15 over time during dialysis. Recombinant bovISG15 was unstable over time in solution based on Coomasie-stained one-dimensional SDS−PAGE (A). The protein formed a dimer after being dialyzed for 4 h. Dialysis for 24 h after storage at −20 °C resulted in the formation of 8.5 and 26 kDa bands, as well as 17 and 34 kDa bands. Formation of rbovISG15 multimers was inhibited during dialysis by reducing [BME (B and C)] or alkylating (iodoacetamide after reduction; data not shown) reagents. Western blots are shown for rbovISG15 (B) in the presence (+) or absence (−) of BME. Multimer formation of rbovISG15 was prevented by the presence of the reductant, reduction and alkylation, or by site-directed mutagenesis of Cys80 to Ser80 (Figure 3). Western blots for rbovISG15 were quantified and analyzed (D). The level of multimer formation increased as time and temperature increased under the oxidizing conditions of dialysis. Note the loss of rbovISG15 (17 kDa) in the absence of BME and the appearance of the 34 kDa dimer, as well as the 24 kDa multimer (Δ) after dialysis for 48 h. Means are different ($p < 0.0001$) when designated with an asterisk.

band appeared (Figure 3C) over time in dialysis and in the absence or presence of BME (Figure 3D). To avoid this expression artifact, *E. coli* extracts were lysed immediately, rather than being stored overnight at 4 °C in subsequent studies that used Cys80Ser ISG15.

Effects of storage (18 days at 4 °C in PBS) of the recombinant proteins were analyzed by MALDI-TOF MS and Western blots (Figure 4). The MALDI-TOF mass spectrum resolved masses of 17 455 and 34 908 Da in the Cys80 rbovISG15, which corresponded to sizes of detected bands in the Western blot analysis (Figure 4A). Site-directed mutagenesis of Cys80Ser rbovISG15 resulted in stability during storage and resolution of a single 17 kDa molecular mass species in the Western blot and the mass spectrum (Figure 4B). Longer-term effects of storage (−20 °C for 1 year in PBS) on the rbovISG15 protein were also examined by MALDI-TOF MS and Western blot analysis. The stored protein was isolated using a C18 ZipTip for mass spectral analysis (data not shown). Many 8 and 26 kDa proteins were observed in the mass spectrum, which did not correspond to

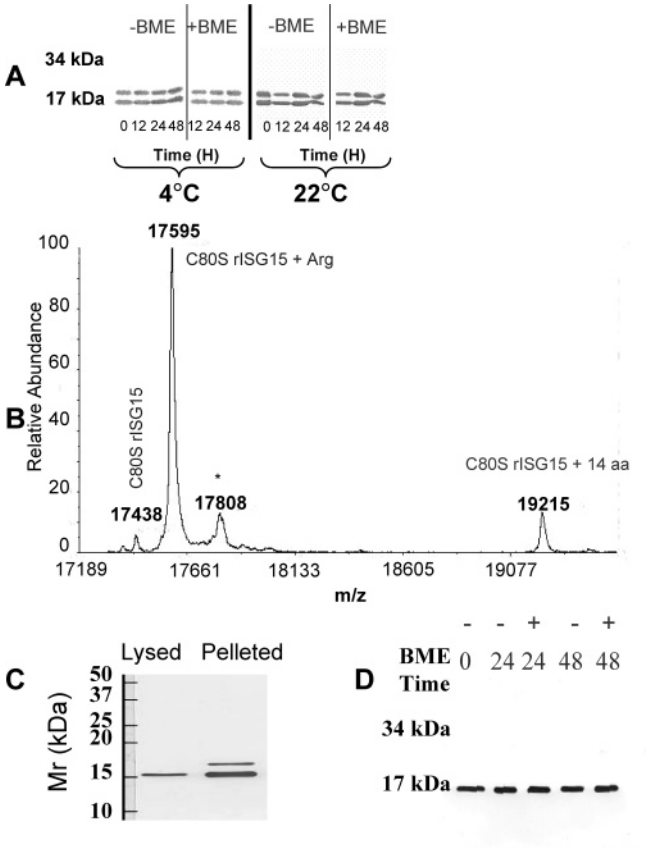

FIGURE 3: MALDI-TOF MS and Western blot analysis of Cys80Ser rbovISG15. Synthesis of Cys80Ser rbovISG15 was confounded by the appearance of a slightly larger form of the protein (A). The Cys80Ser immunoreactive band at 19 kDa was the result of addition of 14 amino acids to the C-terminal end of Cys80Ser rISG15 (confirmed with MALDI-TOF MS, panel B). This was caused by a lack of recognition of a stop codon within the cDNA for rbovISG15, followed by recognition of a double stop codon immediately downstream within the expression vector. When *E. coli* cells were pelleted and stored at 4 °C, two forms of Cys80Ser rbovISG15 were synthesized (see the doublet in panels A and C). However, when the cells were lysed immediately and stored at 4 °C, only the 17 kDa band appeared (C). The matrix adduct for sinapinic acid is indicated with an asterisk. Cys80Ser rbovISG15 existed as a single 17 kDa band that was not affected by BME following dialysis for 24 and 48 h at 22 °C (D).

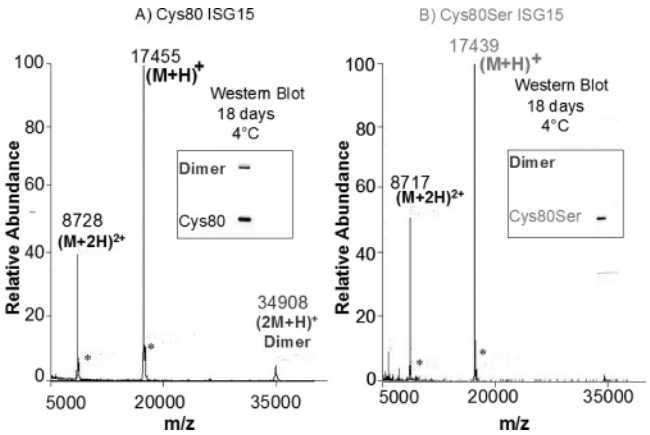

FIGURE 4: MALDI-TOF MS analysis of rbovISG15 and Cys80Ser rbovISG15 in solution. MALDI-TOF MS revealed the parent ions $(M + H)^+$ for rbovISG15 and Cys80Ser rbovISG15. However, the resolved mass for the rbovISG15 dimer (A) was a minor species in the mass spectrum, whereas in the Western blot (inset), it was resolved as a major form of rbovISG15. In contrast, MALDI-TOF MS and Western blots revealed only the 17 kDa form of Cys80Ser rbovISG15 (B). The matrix adduct ion is designated with an asterisk for sinapinic acid.

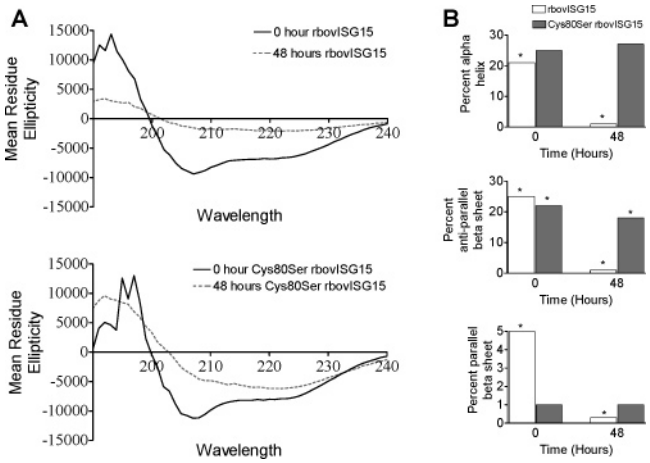

FIGURE 5: Analysis of rbovISG15 secondary structure using circular dichroism spectroscopy. Panel A represents the mean residue ellipticity plot for Cys80 rbovISG15 (top) and Cys80Ser rbovISG15 (bottom) following dialysis for 0 (—) or 48 h (- - -). Secondary structures calculated for the spectra shown in panel A were completed by using the Varslc algorithm (B). These calculations show that the percent α-helix and antiparallel β-sheet diminished over time with dialysis ($p < 0.05$) for Cys80 rbovISG15. In contrast, Cys80Ser rbovISG15 did not exhibit a significant difference for α-helix and parallel β-sheet over time during dialysis. Means differ ($p < 0.05$) when marked with an asterisk.

single fragmentation at a single amino acid along the protein backbone.

Circular Dichroism of Recombinant ISG15 Proteins over Time. Secondary structures of rbovISG15 and Cys80Ser rbovISG15 were compared using circular dichroism spectroscopy as shown in Figure 5A. Proteins were compared after dialysis for 0 and 48 h in 0.01 mM sodium phosphate buffer since secondary structure can be determined only under low-salt conditions by CD spectroscopy. The secondary structure content was calculated with the algorithm Varslc for the spectra collected in Figure 5A and is presented in Figure 5B. α-Helix at 0 h for rbovISG15 (21%) closely resembled the Cys80Ser mutant (25%). The rbovISG15 protein lost α-helical structure after being dialyzed for 48 h ($p < 0.05$). However, Cys80Ser rbovISG15 did not significantly lose secondary structure after being dialyzed for 48 h. The amount of antiparallel β-sheet decreased ($p < 0.05$) in rbovISG15 after 48 h from 25 to 1%. The Cys80Ser antiparallel β-sheet content after no dialysis was 22% and decreased ($p < 0.05$) to 18% after 48 h. The amount of parallel β-sheet decreased ($p < 0.05$) in rbovISG15 from 5% after no dialysis to 0.3% after 48 h. In contrast, the amount of parallel β-sheet (1%) did not change ($p > 0.05$) in the Cys80Ser protein over time during dialysis.

Examination of the effects of dialysis and time on rovISG15 and Cys80Ser rovISG15 by using circular dichroism is shown in Figure 6. Random coil conformation appeared to dominate in both rovISG15 and Cys80Ser rovISG15 spectra after dialysis for 0 and 48 h. Varlsc calculations showed that antiparallel β-sheet structure for rovISG15 was lost ($p < 0.05$) over time compared to that in Cys80Ser rovISG15 (Figure 6B). The level of secondary structure did not change ($p > 0.05$) over time for Cys80Ser

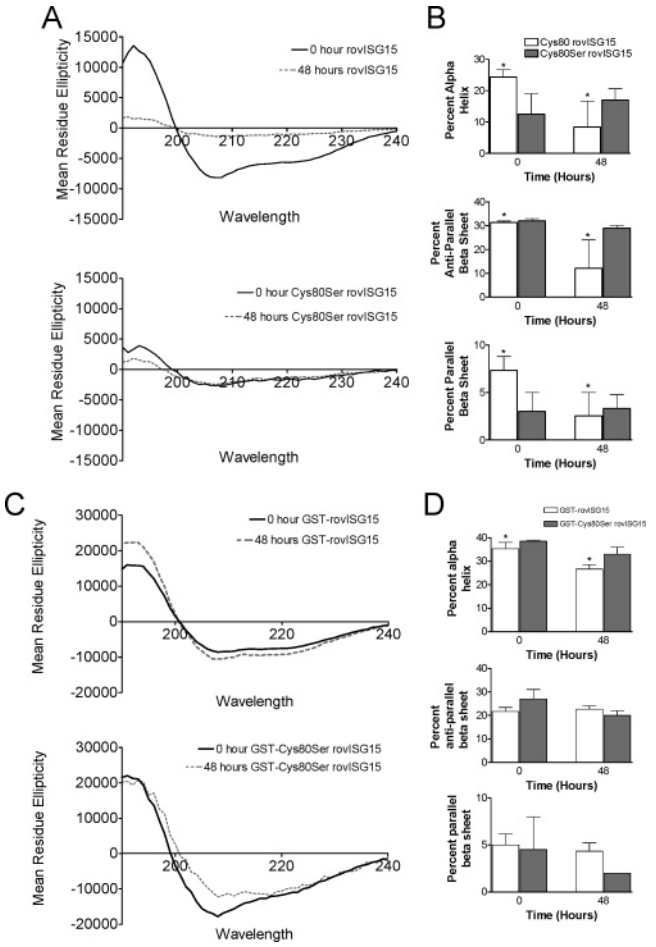

FIGURE 6: Analysis of rovISG15 secondary structure using circular dichroism spectroscopy. The mean residue ellipticity for Cys80 and Cys80Ser ovISG15 following dialysis for either 0 (—) or 48 h (- - -) is shown in panel A. Predicted secondary structure (Varslc) from the plots presented in panel A is shown in panel B. Loss of antiparallel β-sheet over time was more significant for Cys80 when compared with Cys80Ser rovISG15. Also, the total secondary structure of Cys80 showed a significant loss over time with dialysis. Panel C shows the mean residue ellipticity of the GST−ovISG15 and GST−Cys80Ser ovISG15 proteins over time with dialysis. Mean residue ellipticity does not appear significantly different. Calculated secondary structure (Varlsc) for these proteins is shown in panel D. Significant loss of α-helix occurred over time for the GST−rovISG15 protein when compared to that of the GST−Cys80Ser rovISG15 protein. Means differ ($p < 0.05$) when marked with an asterisk.

ovISG15, yet the secondary structure of Cys80Ser rovISG15, based on mean residue ellipticity ($p < 0.05$), was diminished when compared to that of rovISG15 after no dialysis. Recombinant ovISG15 lost ($p < 0.05$) α-helix and parallel β-sheet structure, whereas Cys80Ser rovISG15 did not change over time.

GST fused to the N-terminus of ovine proteins (rovISG15 and Cys80Ser rovISG15) was produced in an effort to examine the stabilizing effects (Figure 6C) and functional consequences of time in dialysis on the proteins. The GST fusion proteins also were required to "pull down" UBE1L via the affinity for GSH−Sepharose. The CD spectra were similar for the GST−rovISG15 fusion protein and Cys80Ser rovISG15. Secondary structure examination by Varslc calculation from the circular dichroism of the dialyzed GST fusion proteins (Figure 6D) revealed no loss ($p > 0.05$) of β-sheet over time for either rovISG15 or the Cys80Ser

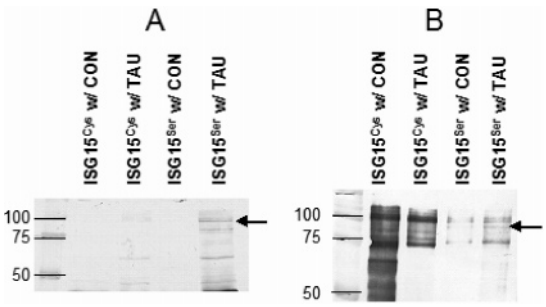

FIGURE 7: Effects of dialysis on the specificity of ovISG15 and Cys80Ser ovISG15 for UBE1L detected by Western blot (10% gel for 0 h and 8% gel for 48 h) with anti-human UBE1L antibody. BEND cell lysates were induced with IFN-τ (or control treated) for production of enzymes specific for ISG15. In panel A, BEND cell lysates were applied to glutathione−Sepharose columns which had Cys80 ovISG15 and Cys80Ser ovISG15 bound at the 0 h dialysis time. Both proteins (0 h dialysis) bind to UBE1L (110 kDa immunoreactive band) in lysates of BEND cells that had been treated with IFN-τ for 24 h. However, following dialysis for 48 h, the more structurally stable Cys80Ser rovISG15 retained greater specificity for interaction with UBE1L (B) when compared to Cys80 rovISG15. The arrow denotes the location of UBE1L within the Western blot.

protein. Loss ($p < 0.05$) of α-helix was revealed in the rovISG15 over time in the Varslc calculation. However, both GST fusion proteins rovISG15 and Cys80Ser rovISG15, based on averaged plots of mean residue ellipticity over time, did not appear to change. Comparison of rovISG15 with Cys80Ser rovISG15 over time in solution showed that loss ($p < 0.001$) of secondary structure occurred for rovISG15 but not Cys80Ser rovISG15 as determined by Varslc calculation.

The Structural Integrity of GST-Fused Ovine Protein Affects Binding to UBE1L. Interaction of GST−rovISG15 and GST−Cys80Ser rovISG15 proteins with UBE1L was examined over time (0 and 48 h) in BEND cell lysates (Figure 7). Interferon-τ induced the binding of GST−rovISG15 and GST−Cys80Ser rovISG15 proteins to UBE1L (immunoreacting band at 110 kDa) after no dialysis (Figure 7A). Cell lysates from nontreated BEND cells did not contain UBE1L. Structural differences for rovISG15 and Cys80Ser rovISG15 affect the ability of rovISG15 to bind UBE1L after dialysis for 48 h (Figure 7B). After being dialyzed for 48 h, rovISG15 bound nonspecifically to many proteins. This was in contrast to Cys80Ser rovISG15, which retained the ability to specifically bind UBE1L after dialysis for 48 h.

Modeling ISG15 and Hinge Region Interactions. Models of native bovISG15, ovISG15, and Cys80Ser ovISG15 were constructed for comparison of the hinge region and structural differences (Figure 8). These models were based on the human Cys78Ser ISG15 crystal structure (1Z2M) of Narasimhan et al. (*14*). bovISG15 had a shorter hinge region (residues 76−80) than ovISG15 or human ISG15 (residues 76−83), thus limiting space between the ubiquitin-like domains.

The averaged secondary structure for modeled bovISG15 had 16% α-helix, 25% β-sheet, 33% turn, and 23% coil. In contrast, ovISG15 had 13% α-helix, 22% β-sheet, 38% turn, and 23% coil. Cys80Ser ovISG15 had 15% α-helix, 23% β-sheet, 35% turn, and 23% coil. Human Cys78Ser ISG15 showed little variation over time in secondary structure (16% α-helix, 23% β-sheet, 28% turn, and 25% coil). The modeled hydrophobic surface area was as follows: human Cys78Ser

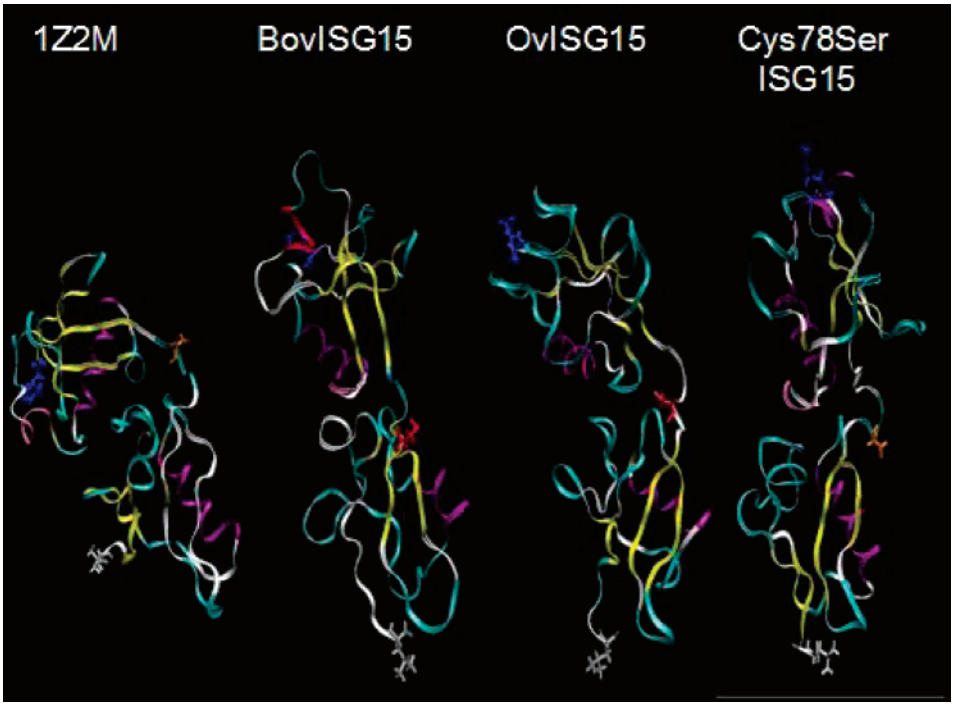

FIGURE 8: Molecular dynamic simulation of 1Z2M, bovISG15, ovISG15, and Cys78Ser ovISG15 (from left to right) with aligned and assigned secondary structure. All models were aligned in the second ubiquitin-like domain of residues 90−140; note that the orientation of the ubiquitin-like domains differs for each model. Colors in bond mode are as follows: blue for residue 3 in 1Z2M and residue 1 in other models, silver for residue 154 in 1Z2M, residue 149 in bovISG15, and residue 152 of Cys78Ser ovISG15, red for Cys78, and orange for Ser78. Secondary structure is indicated in ribbons with the following colors: purple for α-helix, yellow for β-sheet, cyan for turn, tan for β-bridge, mauve for 3−10 α-helix, red for π-helix, and white for coil.

ISG15 with 30.1%, ovISG15 with 34.0%, Cys78Ser ovISG15 with 34.3%, and bovISG15 with 34.7%.

DISCUSSION

The stability of rbovISG15 in solution was examined at 4 °C over a period of 18 days and compared by Western blot analysis and MALDI-TOF MS. Dimer formation was detected using MALDI-TOF MS showing a relatively low abundance (3%) compared to Western blot analysis (30%). The difference in mass spectral abundance may be explained by gas phase fragmentation of the rbovISG15 dimer, differences in ionizing the dimer versus the monomer, concentration effects of the dimer versus the matrix, or crystallization of the dimer within the matrix (*36*). Although MALDI-TOF MS does not provide conclusive results about the relative abundance of the dimer, under similar mass spectral conditions (i.e., concentration, matrix, time, temperature, and laser power), the Cys80Ser rbovISG15 did not show a resolved dimer in the mass spectrum. The ionizing ability of rbovISG15 versus Cys80Ser rbovISG15 may account for this difference. This difference may also reflect structural differences present in the gas phase ions that are produced by mass spectrometry. For instance, folding of rbovISG15 and a hydrophobic hinge region may allow a greater amount of protein−protein interactions than the folded Cys80Ser rbovISG15 when they are ionized. Regardless, detection by Western blot analysis provides evidence that Cys80 is required to promote dimer formation in solution.

Stored rbovISG15 exhibited multimer formation that was detected by Western blot analysis and MALDI-TOF MS. Elution of the proteins with a C18 ZipTip and MALDI-TOF MS revealed that several 8 and 26 kDa proteins were present in the mixture. These rISG15 multimers did not correlate with a recognizable fragmentation, such as single-amino acid cleavage of the protein due to proteolytic activity or interactions that promote irreversible cleavage and dimerization in the absence of a cross-linking reagent. Protein−protein interactions in which nonspecific interactions cause fragmentation of rbovISG15 in solution might contribute to the instability when compared with the more stable Cys80Ser rbovISG15.

Formation of dimers occurred with the rbovISG15 in 0.25 mM Tris, PBS, or 10 mM sodium phosphate over the same period of time at 22 °C. Thus, dimer formation was not due to specific ionic or hydrophobic interactions alone, since ionic strength or buffer had no apparent effect. However, three different lines of evidence show that Cys80 has a role in the formation of these unusual products. First, the presence of a reducing agent (BME) prevented formation of rbovISG15 multimers over time (by 48 h) and at room temperature (22 °C) as shown with Western blots. Second, Cys80Ser rbovISG15 did not change in molecular mass (i.e., form dimers) over time and temperature in the absence of reductant. Third, carboxyamidomethylation of cysteine prevented multimer formation over 48 h. Since the dimers and other products are prevented by these changes, the involvement of cysteine other than formation of disulfide bridges must be considered. If protein−protein interactions can occur in such a way as to assist in the formation of a thiolate ion from Cys80 by reducing its pK_a, this thiolate ion would be able to act as a strong nucleophile for the formation of other coordinate interactions or for promotion of peptide bond hydrolysis.

Changes in secondary structure over time were examined by circular dichroism spectroscopy for an explanation of the behavior of the recombinant proteins in solution. Our results suggest that the cysteine residue contributes to the instability of rbovISG15, whereas the serine residue promotes some secondary structure stability over time in solution. These differences in secondary structure during dialysis of rbovISG15 suggest that folding of the protein changes over time. This instability in solution might explain why we have been unable to improve sensitivity for a rbovISG15 ELISA below 1 ng/mL (not shown).

Recombinant bovISG15 was generated using baculovirus (not shown), yeast (*37*), and *E. coli* (this study) expression systems. None of these recombinant proteins were capable of interacting with UBE1L in extracts derived from BEND cells that were treated with IFN-τ. This was disappointing and thought to be due to the instability of rbovISG15 in solution. In contrast, ovISG15 (87% identical to bovISG15 in sequence) has a longer hinge region (*38*), which was thought to provide better separation of the two ubiquitin-like domains, and better interaction with UBE1L in solution.

Under similar experimental conditions, rovISG15 and Cys80Ser rovISG15 did not exhibit dimer formation after dialysis for 48 h by Western blot or mass spectrometry. Spectral characterization of the ovine proteins by circular dichroism showed that rovISG15 did lose some secondary structure over time relative to Cys80Ser rovISG15. However, the loss of secondary structure for rovISG15 was not as great as that exhibited by Cys80 bovISG15. This propensity for increased stability after site-directed mutagenesis of Cys78 to Ser was noted by Narasimhan (*14*) for human Cys78Ser ISG15 when compared to human ISG15. This work also modeled the structure of ISG15 with UBE1L and noted that the C-terminal ubiquitin-like region of ISG15 interacted with UBE1L. Circular dichroism of human ISG15 and Cys78Ser human ISG15 by Narasimhan (*14*) showed little variation in the amount of α-helix and β-sheet present within these proteins.

Structural integrity over time for the hinge region appeared to play a strong role in the ability to bind ISG15 to UBE1L. Recombinant ovISG15 was able to bind UBE1L after no dialysis, whereas rbovISG15s (Cys80 and Cys80Ser) were unable to bind UBE1L. Recombinant ovISG15 did show loss of secondary structure after dialysis for 48 h and the apparent ability to specifically bind UBE1L. However, the site-directed mutant Cys80Ser rovISG15 maintained structure and was able to bind UBE1L, even after being dialyzed for 48 h. This trend implies that Cys80 has a destabilizing effect on the region involved in binding UBE1L, which would correlate with the work of Narasimhan (*14*). A possible scenario for Ser80 then involves hydrogen bonding which stabilizes the hinge region and promotes exposure of the C-terminal RLRGG sequence to target molecules.

Typically, under oxidizing conditions, cysteine residues stabilize the protein by forming disulfide bonds (*39*, *40*). However, other molecular interactions may dominate over time in solution, which promotes complex formation in rbovISG15. Our results show that the stronger reductant (BME) prevented rbovISG15 from forming a precipitate over time in solution, whereas Narasimhan et al. (*14*) was unable to prevent precipitation of human ISG15 with 10 mM DTT. In support of this interpretation, experimental conditions (no reductant, extended dialysis) which promoted dimer formation in rbovISG15 did not produce multimers in Cys80Ser rbovISG15. In addition, mutation of the Cys within the hinge region to Ser could have stabilized the secondary structure via hydrogen bonding and prevented protein−protein interactions, which were observed in rISG15. Circular dichroism provided supporting evidence that showed that Cys80Ser rbovISG15 did not change much structurally over time, whereas rbovISG15 lost all secondary structure by 48 h in solution.

During dialysis, the Cys80Ser rovISG15 secondary structure changed the least over time (Varslc calculation) compared to that of rovISG15. Site-directed mutagenesis may have increased the number of hydrogen bonds within the hinge region for the ovine protein and stabilized the secondary structure, thus maintaining a viable protein for binding UBE1L. Cysteine 80 in rovISG15 over time did have an effect structurally that weakened the specific binding to UBE1L after dialysis. Thus, structural integrity about the hinge region has an effect on the biological activity of ISG15.

Models of bovISG15 and ovISG15 were based on the crystal structure of human Cys78Ser ISG15 (*14*). These models revealed distinct changes in structure that may contribute to differences in function of rbovISG15 and rovISG15 examined in this study. The shorter hinge region of bovISG15 may have greater intramolecular interactions than ovISG15. In addition, the interactions between the ubiquitin-like domains would be greater in number in bovISG15 and could change the orientation of the ubiquitin-like domain responsible for binding UBE1L. The decreased mobility of the hinge region, like that of Cys80Ser ovISG15, may prevent structural instability over time which promotes the conjugation of ISG15 to UBE1L.

In summary, rbovISG15 is unstable over time in storage and dialysis. In vivo, conjugation of ISG15 to targeted proteins occurs inside the cell, which is within a slightly reducing environment. Also, because ISG15 retains a conserved Cys within the hinge region across several species, we postulate that it might contribute to the instability of the protein. Site-directed mutagenesis and chemical modification of cysteine stabilize rbovISG15 on the basis of Western blot analysis, MALDI-TOF MS, CD spectroscopy, and molecular dynamics modeling. This mutation is affected by differences in spacing in the hinge region and the orientation of the ubiquitin-like domains. We conclude that Cys80 contributes to the instability of rbovISG15 in solution but that this is not due to formation of a disulfide bond. Rather, it is postulated that Cys80, via nucleophilic attack and its proximity to one of the ubiquitin-like domains, forms a covalent attachment with an acceptor amino acid (e.g., Lys or Gly) to form a dimer over time in storage or dialysis. Finally, the hinge region Cys and spacing between the ubiquitin domains contribute to the structure and function of rISG15 in solution.

SUPPORTING INFORMATION AVAILABLE

Movies from the aligned simulated models (using the color scheme described in Figure 8) of ovISG15, Cys78Ser ovISG15, and bovISG15 are available free of charge via the Internet at http://pubs.acs.org.

REFERENCES

1. Finley, D., and Chau, V. (1991) Ubiquitination, *Annu. Rev. Cell Biol. 7*, 25−69.
2. Pickart, C. M. (2001) Mechanisms underlying ubiquination, *Annu. Rev. Biochem. 70*, 503−33.
3. Wilkinson, K. D., Ventii, K. H., Friedrich, K. L., and Mullally, J. E. (2005) The ubiquitin signal: Assembly, recognition and termination. Symposium on ubiquitin and signaling, *EMBO Rep. 6*, 815−20.
4. Schwartz, A. L., and Ciechanover, A. (1999) The ubiquitin-proteasome pathway and pathogenesis of human diseases, *Annu. Rev. Med. 50*, 57−74.
5. Ross, C. A., and Pickart, C. M. (2004) The ubiquitin-proteasome pathway in Parkinson's disease and other neurodegenerative diseases, *Trends Cell Biol. 14*, 703−11.
6. Haas, A. L., Warms, J. V., Hershko, A., and Rose, I. A. (1982) Ubiquitin-activating enzyme. Mechanism and role in protein-ubiquitin conjugation, *J. Biol. Chem. 257*, 2543−8.
7. Hershko, A., Heller, H., Elias, S., and Ciechanover, A. (1983) Components of ubiquitin-protein ligase system. Resolution, affinity purification, and role in protein breakdown, *J. Biol. Chem. 258*, 8206−14.
8. Pickart, C. M., and Rose, I. A. (1985) Functional heterogeneity of ubiquitin carrier proteins, *J. Biol. Chem. 260*, 1573−81.
9. Wilkinson, K. D., and Hochstrasser, M. (1998) *The deubiquinating enzymes*, 1st ed., Plenum Press, New York.
10. Haas, A. L., Ahrens, P., Bright, P. M., and Ankel, H. (1987) Interferon induces a 15-kilodalton protein exhibiting marked homology to ubiquitin, *J. Biol. Chem. 262*, 11315−23.
11. Loeb, K. R., and Haas, A. L. (1992) The interferon-inducible 15-kDa ubiquitin homolog conjugates to intracellular proteins, *J. Biol. Chem. 267*, 7806−13.
12. Yuan, W., and Krug, R. M. (2001) Influenza B virus NS1 protein inhibits conjugation of the interferon (IFN)-induced ubiquitin-like ISG15 protein, *EMBO J. 20*, 362−71.
13. Rempel, L. A., Francis, B. R., Austin, K. J., and Hansen, T. R. (2005) Isolation and sequence of an interferon-tau-inducible, pregnancy- and bovine interferon-stimulated gene product 15 (ISG15)-specific, bovine ubiquitin-activating E1-like (UBE1L) enzyme, *Biol. Reprod. 72*, 365−72.
14. Narasimhan, J., Wang, M., Fu, Z., Klein, J. M., Haas, A. A., and Kim, J. J. (2005) Crystal structure of the interferon-induced ubiquitin-like protein ISG15, *J. Biol. Chem. 280*, 27356−65.
15. Johnson, G. A., Spencer, T. E., Hansen, T. R., Austin, K. J., Burghardt, R. C., and Bazer, F. W. (1999) Expression of the interferon tau inducible ubiquitin cross-reactive protein in the ovine uterus, *Biol. Reprod. 61*, 312−8.
16. Hansen, T. R., Austin, K. J., and Johnson, G. A. (1997) Transient ubiquitin cross-reactive protein gene expression in the bovine endometrium, *Endocrinology 138*, 5079−82.
17. Austin, K. J., Ward, S. K., Teixeira, M. G., Dean, V. C., Moore, D. W., and Hansen, T. R. (1996) Ubiquitin cross-reactive protein is released by the bovine uterus in response to interferon during early pregnancy, *Biol. Reprod. 54*, 600−6.
18. Austin, K. J., Pru, J. K., and Hansen, T. R. (1996) Complementary Deoxyribonucleic Acid Sequence Encoding Bovine Ubiquitin Cross-Reactive Protein, *Endocrine 5*, 191−7.
19. Austin, K. J., Bany, B. M., Belden, E. L., Rempel, L. A., Cross, J. C., and Hansen, T. R. (2003) Interferon-Stimulated Gene-15 (Isg15) Expression is Upregulated in the Mouse Uterus in Response to the Implanting Conceptus, *Endocrinology 144*, 3107−13.
20. Johnson, G. A., Joyce, M. M., Yankey, S. J., Hansen, T. R., and Ott, T. L. (2002) The Interferon Stimulated Genes (ISG) 17 and Mx have different temporal and spatial expression in the ovine uterus suggesting more complex regulation of the Mx gene, *J. Endocrinol. 174*, R7−11.
21. Bebington, C., Bell, S. C., Doherty, F. J., Fazleabas, A. T., and Fleming, S. D. (1999) Localization of ubiquitin and ubiquitin cross-reactive protein in human and baboon endometrium and decidua during the menstrual cycle and early pregnancy, *Biol. Reprod. 60*, 920−8.
22. Hamerman, J. A., Hayashi, F., Schroeder, L. A., Gygi, S. P., Haas, A. L., Hampson, L., Coughlin, P., Aebersold, R., and Aderem, A. (2002) Serpin 2a is induced in activated macrophages and conjugates to a ubiquitin homolog, *J. Immunol. 168*, 2415−23.
23. Malakhov, M. P., Kim, K. I., Malakhova, O. A., Jacobs, B. S., Borden, E. C., and Zhang, D. E. (2003) High-throughput immunoblotting: Ubiquitin-like protein ISG15 modifies key regulators of signal transduction, *J. Biol. Chem. 278*, 16608−13.
24. Malakhova, O. A., Yan, M., Malakhov, M. P., Yuan, Y., Ritchie, K. J., Kim, K. I., Peterson, L. F., Shuai, K., and Zhang, D. E. (2003) Protein ISGylation modulates the JAK-STAT signaling pathway, *Genes Dev. 17*, 455−60.
25. Zhao, C., Denison, C., Huibregtse, J., Gygi, S., and Krug, R. (2005) Human ISG15 conjugation targets both IFN-induced and constitutively expressed proteins functioning in diverse cellular pathways, *Proc. Natl. Acad. Sci. U.S.A. 102*, 10200−5.
26. Narasimhan, J., Potter, J. L., Haas, A. L., Ahrens, P., Bright, P. M., and Ankel, H. (1996) Conjugation of the 15-kDa interferon-induced ubiquitin homolog is distinct from that of ubiquitin, *J. Biol. Chem. 271*, 324−30.
27. Austin, K. J., Carr, A. L., Pru, J. K., Hearne, C. E., George, E. L., Belden, E. L., and Hansen, T. R. (2004) Localization of isg15 and conjuated proteins in bovine endometrium using imunohistochemistry and electron microscopy, *Endocrinology 145*, 967−75.
28. Manavalan, P., and Johnson, W. C. J. (1987) Variable selection method improves the prediction of protein secondary structure from circular dichroism spectra, *Anal. Biochem. 167*, 76−85.
29. Lobley, A., and Wallace, B. A. (2001) DICHROWEB: A website for the analysis of protein secondary structure from circular dichroism spectra, *Biophys. J. 80*, 373a.
30. Lobley, A., Whitmore, L., and Wallace, B. A. (2002) DICHROWEB: An inreactive website for the analysis of protein secondary structure from circular dichroism spectra, *Bioinformatics 18*, 211−2.
31. Schwede, T., Kopp, J., Guex, N., and Peitsch, M. C. (2003) SWISS-MODEL: An automated protein homology-modeling server, *Nucleic Acids Res. 31*, 3381−5.
32. Brooks, B. R., Bruccoleri, R. E., Olafson, B. D., States, D. J., Swaminathan, S., and Karplus, M. (1983) CHARMM: A program for macromolecular energy, minimization, and dynamics calculations, *J. Comput. Chem. 4*, 187−217.
33. Laxmikant, K., Skeel, R., Bhandarkar, M., Brunner, R., Gursoy, A., Krawetz, N., Phillips, J., Shinozaki, A., Varadarajan, K., and Schulten, K. (1999) NAMD2: Greater scalability for parallel molecular dynamics, *J. Comput. Phys. 151*, 283−312.
34. Humphrey, W. F., Dalke, A., and Schulten, K. (1996) VMD visual molecular dynamics, *J. Mol. Graphics 14*, 33−8.
35. Frishman, D., and Argos, P. (1995) Knowledge-based protein secondary structure, *Proteins 23*, 566−79.
36. Cohen, L. R. H., Strupat, K., and Hillenkamp, F. (1997) Analysis of Quaternary Protein Ensembles by Matrix Assisted Laser Desorption/Ionization Mass Spectromet, *J. Am. Soc. Mass Spectrom. 8*, 1046−52.
37. Pru, J. K., Austin, K. J., Perry, D. J., Nighswonger, A. M., and Hansen, T. R. (2000) Production, purification, and carboxy-terminal sequencing of bioactive recombinant bovine interferon-stimulated gene product 17, *Biol. Reprod. 63*, 619−28.
38. Nighswonger, A. M., Austin, K. J., Ealy, A. D., Han, C. S., and Hansen, T. R. (2000) Rapid communication: The ovine cDNA encoding interferon-stimulated gene product 17 (ISG17), *J. Anim. Sci. 78*, 1393−4.
39. Jacob, C., Giles, G. I., Giles, N. M., and Sies, H. (2003) Sulfur and selenium: The role of oxidation state in protein structure and function, *Angew. Chem., Int. Ed. 42*, 4742−58.
40. Giles, N. M., Watts, A. B., Giles, G. I., Fry, F. H., Littlechild, J. A., and Jacob, C. (2003) Metal and Redox Modulation of Cysteine Protein Function, *Chem. Biol. 10*, 677−93.

BI061408X